REPORT

OF

PORT AND HARBOUR RESEARCH INSTITUTE

REPORT NO. 12

On the f^{-5} Law of Wind—Generated Waves

——An experimental supplement——

by

Tokuichi Hamada

A Note on the Development of Wind Waves in an Experiment

by

Tokuichi Hamada, Akihiko Shibayama, Hajime Kato

June 1966

PORT AND HARBOUR RESEARCH INSTITUTE

MINISTRY OF TRANSPORT

1-1, 3 Chome, Nagase Yokosuka-City, Kanagawa-Prefecture, Japan

CONTENTS

ON THE f^{-5} LAW OF WIND-GENERATED WAVES

— An experimental supplement —

Contents

風波の f^{-5} 則について

——実験による補足——

浜田徳一

概　要

風波の f^{-5} 則についてはさきに英文報告第6号によりその解析的考察を発表し，また無風状態の水域を通過する風波による実験結果を報告した。今回の補足は風の直接作用を受けている状態の風波につき，その波形スペクトルムの高周波成分がどの様な変化を行うかを実験的に考察したものであり，その解析結果は英文報告第6号に示した見解を支持している。

ON THE f^{-5} LAW OF WIND-GENERATED WAVES

—— An experimental supplement ——

Tokuichi Hamada*

Abstract

The frequency spectra of the wave profile are measured for wind waves generated by the air flow on water surface in a waterway, in which the depth of water is taken 15 cm and 3 cm respectively. Waves are sustained at stationary states. The analysis of the high frequency part of these spectra (the high frequency part means components which have the higher frequency than the frequency of the peak intensity of spectrum) has been made in connection with author's view of the characteristics of the spectrum, which are revealed when the expression $E(f)\sim f^{-n}$ indicates $n>5$ in the case of deep water.

The results of analysis of experimental data show that, (i) the intensity of high frequency part of the spectrum changes progressively its value from windward to leeward in closely correlated forms with the value of n, and (ii) the attenuation coefficient of the intensity of high frequency part concerned with the running distance of wave energy has similar values in both cases of wind waves under the direct wind action and of wind-generated waves in the calm condition, when the value of n becomes 7~10 in like manner.

§ 1. Introduction

We call the paper "On the f^{-5} law of wind-generated waves" (T. Hamada (1964)) as Paper (I), and in this paper we pursue experimentally the equilibrium problem of high frequency part of the frequency spectrum of wave profile in succession of Paper (I). The depth of water to bottom is finite in the present experiment, and the analysis generally needs the treatment of cases of the finite depth. But, in the region treated in this paper, the high frequency part of the spectrum may be possible to be considered as the case of deep water approximately. The author already showed that the unstable attenuation may occur in the concerned part of the spectrum, if n is greater than 5 in the expression $E(f)\sim f^{-n}$ of the high frequency part of the frequency spectrum of wind-generated waves in deep weter. This phenomenon does not need the existence of surface instability, and the cause is attributed to the transfer of wave energy to some vortex motion.

* Chief, Hydraulics Laboratory, Hydraulics Division.

The same phenomenon may occur in the case of wind wave which is developing under the direct action of air flow. In this case the surface of waves is covered by the well developed capillary waves, and the crests of waves are often breaking. These surface properties may be also influential to the behavior of the high frequency part of the frequency spectrum of wave profile. Our experimet shows that even in this case the unstable attenuation pointed out in Paper (I) is clearly effective in the high frequency part of the spectrum.

§ 2. Experiments

The waterway used in this experiment is same as that in Paper (I). In the present case the depth of water to bottom is taken 3cm and also 15cm, and the shape of cross section of air flow on water surface is same in both cases. The width of waterway is 150cm, and so the effect of side friction to waves is far smaller than the effect of bottom friction.

The characteristics of air flow are shown by Table—1 (depth of water 3cm) and by Table—2 (depth of water 15cm). The air flow thus examined runs over the total length of the waterway, and is not excluded in a midway. The shearing stress on the water surface recorded in these tables has been obtained by the assumption of logarithmic law of wind profile. In the case of water depth 15cm, the wave height is relatively large, and the wind profile near the water surface cannot be determined accurately. Stillmore the direct application of the logarithmic law to the lowest layer of air flow may have some doubt, and so we used the wind profile at rather high stations. The shearing stress in this case may have possibility to be overestimated in some degree.

In Table—1 and 2 stations Ba, Ca and Da situate 965cm, 1865cm and 2765cm leeward in order from the section where air flow begins to contact the water surface initially. U_{1000cm} (cm/sec) and $r^2{}_{1000cm}$ are obtained by the assumption of the logarithmic law for the height of 1000cm. U_{40cm} (cm/sec) is the measured value in the middle height of air flow. U_{40cm} in both tables is nearly equal at *r. p. m.* 400 of air blower. This suggests that U_{40cm} does not vary indifferent to the change of the depth of water at the same r. p. m. of air blower. But τ_0 (dyne/cm^2) and U_* (cm/sec) vary with the change of the depth of water. The case of *r. p. m.* 400 of air blower in both tables shows a good example.

In these experiments water on the bottom plate is drifted leeward by wind, and is compesnsated by its windward creep through the layer under the bottom

Table—1 Characteristics of air flow at the depth of water 3 cm

Station	r.p.m.	τ_0 dyne/cm^2	U_* cm/s	z_0 cm	U_{1000cm} cm/s	U_{40cm} cm/s	γ^2_{1000cm}	$z_0/H_{1/3}$ mean	$H_{1/3}$ mean, cm	L cm	ρ_a
				$\times 10^{-3}$			$\times 10^{-3}$				$\times 10^{-3}$
	200	0.874	27.13	10.8	775	545	1.226			35	1.187
	200	0.880	27.30	10.9	779	551	1.228	0.0161	0.621	75	1.181
	200	0.784	25.74	8.30	752	546	1.172			115	1.183
	300	1.62	36.78	5.68	1109	826	1.099			35	1.196
B_a	300	1.58	36.52	5.18	1110	849	1.082	0.0083	0.768	75	1.187
	300	1.53	35.83	8.26	1047	847	1.171			115	1.189
	400	2.35	44.35	2.70	1420	1120	0.975			35	1.196
	400	2.38	44.52	3.02	1413	1131	0.993	0.0046	0.758	75	1.202
	400	2.32	44.17	4.82	1350	1136	1.070			115	1.188
	200	0.692	23.83	3.80	742	586	1.030			35	1.219
	200	0.700	24.35	3.44	765	592	1.013	0.0054	0.812	75	1.212
	200	0.684	23.83	5.94	716	594	1.108			115	1.204
	300	1.41	34.09	2.12	1112	882	0.940			35	1.212
C_a	300	1.48	34.78	2.24	1130	904	0.947	0.0022	0.886	75	1.220
	300	1.18	31.30	1.56	1045	878	0.897			115	1.204
	400	2.73	47.83	3.10	1515	1176	0.997			35	1.193
	400	2.90	49.22	3.50	1544	1205	1.016	0.0032	1.025	75	1.195
	400	2.51	45.56	3.24	1438	1182	1.004			115	1.208

: L means the distance of lateral direction from the frontal side wall of waterway.

Table—2 Characteristics of air flow at the depth oh water 15 cm

Station	r.p.m.	τ_0 dyne/cm^2	U_* cm/s	z_0 cm	U_{1000cm} cm/s	U_{40cm} cm/s	γ^2_{1000cm}	$z_0/H_{1/3}$ mean	$H_{1/3}$ mean, cm	L cm	ρ_a
							$\times 10^{-3}$				$\times 10^{-3}$
	400	10.87	96.0	0.22	2010	1195	2.28			35	1.180
B_a	400	11.76	100.2	0.24	2080	1199	2.31	0.0432	4.32	75	1.172
	400	8.82	87.0	0.10	2000	908	1.89			115	1.167
	400	9.13	88.0	0.22	1853	1156	2.25			35	1.179
C_a	400	8.18	83.3	0.13	1860	1219	2.00	0.0251	5.77	75	1.179
	400	7.76	81.0	0.087	1895	1215	1.82			115	1.184
	400	6.60	75.0	0.047	1870	1229	1.60			35	1.174
D_a	400	7.56	80.4	0.074	1907	1296	1.77	0.0072	6.37	75	1.171
	400	5.13	66.3	0.017	1815	1238	1.33			115	1.169

plate. Therefore the relatively strong uniform water current is induced by the increase of wind velocity especially in the case of the depth of water 3cm. The order of the velocity of this current will be estimated later. As the current is induced, the change of water level at the presence of wind is small, and is practically neglected. Table—3 shows the change of waterlevel.

Table—3 The change of water level

Station	r. p. m. 200	r. p. m. 300	r. p. m. 400
B_W	− 1.2 mm	− 2.2	− 2.8
C_W	− 0.5	− 0.8	− 1.0
D_W	+ 0.3	+ 0.4	+ 0.6

: the depth of water to bottom 3 cm

The main characteristics of waves generated by the air flow are recorded in Table—4 and 5. The stations Bw, Cw and Dw for the measurement of wave

profile situate 10cm leeward to Ba, Ca and Da respectively. Records in Table—4, —5 are all obtained by the representation of frequency spectrum of wave profile at the stationary state. As shown in Paper (I) the spectrum used in this paper is the average of 9 original spectra, in which each has $N=36$ in χ^2 —freedom, and is taken equally at the middle and its both sides of the same section.

Table—4 Wave dimensions at the depth to bottom 3 cm

Station	r. p. m.	$\overline{\eta^2}$ cm²	$H_{1/3}$ cm	$\overline{f}_{zero\ up\text{-}cross}$ c/s	$\overline{f}_{Max}$ c/s	$f_{peak\ of\ spectrum}$ c/s	ε	$\frac{f_{peak\ of\ spectrum}}{\overline{f}_{zero\ up\text{-}cross}}$
B_W	200	0.0241	0.621	5.19	5.36	5.00	0.258	0.963
	300	0.0368	0.768	4.53	4.94	4.20	0.400	0.928
	400	0.0358	0.758	5.39	6.41	4.40	0.541	0.817
C_W	200	0.0411	0.812	4.12	4.75	3.60	0.496	0.874
	300	0.0490	0.886	4.02	4.70	3.40	0.520	0.847
	400	0.0655	1.025	5.00	6.36	3.90	0.617	0.781

Table—5 Wave dimensions at the depth to bottom 15 cm

Station	r. p. m.	$\overline{\eta^2}$ cm²	$H_{1/3}$ cm	$\overline{f}_{zero\ up\text{-}cross}$ c/s	$\overline{f}_{Max}$ c/s	$f_{peak\ of\ spectrum}$ c/s	ε	$\frac{f_{peak\ of\ spectrum}}{\overline{f}_{zero\ up\text{-}cross}}$
B_W	400	1.166	4.32	2.72	3.19	2.45	0.521	0.90
C_W	400	2.094	5.77	2.12	2.40	1.95	0.464	0.92
D_W	400	2.547	6.37	1.84	2.16	1.65	0.525	0.90

: Here

$$\overline{f}_{zero\ up\text{-}cross} = \left\{\frac{m_2}{m_0}\right\}^{\frac{1}{2}}$$

$$\overline{f}_{Max} = \left\{\frac{m_4}{m_2}\right\}^{\frac{1}{2}}$$

$$\varepsilon = \left\{\frac{m_0 m_4 - m^2_2}{m_0 m_4}\right\}^{\frac{1}{2}}$$

$$m_n = \int_0^\infty f^n E(f)\,df$$

A noticeable point is that the records of frequencies in Table—4 are probably influenced by the water current induced by wind. Then we make a table (Table—6) of $c^{(1)}$, $c^{(2)}$, $c^{(2)}/c^{(1)}$ and $\alpha_1 = \sec^{-1}\frac{c^{(2)}}{c^{(1)}}$ at the case of the depth of water 3cm using a same method as Table—1 of Paper (I). α_1 in Table—6 is greater than the corresponding value in Table—1 of Paper (I), and it increases with the increase of the velocity of wind, though the case of r. p. m. 200 of blower in Table—6 indicates the value very near to those in Paper (I). Therefore we may think that the appeared increase of α_1 in Table—6 is caused by the influence of the drift current, which increases the observed frequency of the wave of the same wave number, and strengthens the appeared celerity of wave crest along the side wall of waterway.

Table—6 Appeared celerities (depth of water 3 cm)

r. p. m.	Station	$c^{(1)}$ cm/sec	$c^{(2)}$ cm/sec	$c^{(2)}/c^{(1)}$	$\alpha_1=\sec^{-1}\frac{c^{(2)}}{c^{(1)}}$
200	B_W	32.2	49.1	1.52	49°
200	C_W	37.9	56.7	1.50	48°02′
300	B_W	35.5	57.7	1.63	52°02′
300	C_W	38.5	62.7	1.63	52°08′
400	B_W	31.4	65.6	2.09	61°25′
400	C_W	33.1	70.4	2.13	61°58′

: $c^{(1)}$ means phase velocity of wave corresponding to $\bar{f}_{\text{zero up-cross.}}$
$c^{(2)}$ means the average value of translation celerity of appeared wave crest along the side wall.

We virtually assume that the induced water current has an uniform velocity distribution (U_U), and that the representative direction of progress of waves intersects the side wall of waterway with an angle α. Using $c^{(2)}$ (appeared celerity of wave along the side wall of waterway) and $c_0^{(1)}$ (real celerity of the same wave in still water).

$$\frac{c^{(2)}-U_U}{c_0^{(1)}}=\sec\alpha \qquad (1)$$

$$\frac{c_0^{(1)}+U_U\cos\alpha}{f}=\frac{2\pi}{k} \qquad (2)$$

$$c_0^{(1)} = \left\{ \frac{g + T'k^2}{k} \tanh k h \right\}^{\frac{1}{2}} \qquad (3)$$

From the relation (2), the frequency of the same wave in still water is

$$f_0 = f - U_U \cos\alpha \cdot \frac{k}{2\pi} \qquad (4)$$

we modify $\overline{f}_{zero\ up\text{-}cross}$ in Table—4 to $(\overline{f}_{zero\ up\text{-}cross})_0$ in still water using above relations. Directional angle α may be assumed in this treatment. Using the relation $c^{(2)}/c^{(1)} = \sec\alpha$ ($c^{(1)} = c_0^{(1)} + U_U \cos\alpha$), the value of $c^{(2)}/c^{(1)}$ is assumed as 1.40 in every case. This trial is made in the references of Table—1 of Paper (I) and of the case of r. p. m. 200 in Table—6 of this paper. So α is 44° 25′. Following to the numerical procedure modified frequency in still water is obtained, and it is shown in Table—7 with other usable physical values.

Table—7

depth to bottom	r. p. m.	Station	$\overline{f}_{zero\ up\text{-}cross}$ c/s	$(\overline{f}_{zero\ up\text{-}cross})_0$ c/s	U_U cm/sec	h/L	$H_{1/3}/L$
3 cm	200	B_W	5.19	4.94	2.34	$\frac{1}{2.25}$	$\frac{1}{10.87}$
	200	C_W	4.12	3.96	2.20	$\frac{1}{3.27}$	$\frac{1}{12.11}$
	300	B_W	4.53	4.14	4.97	$\frac{1}{3.03}$	$\frac{1}{11.85}$
	300	C_W	4.02	3.66	5.62	$\frac{1}{3.71}$	$\frac{1}{12.59}$
	400	B_W	5.39	4.26	13.75	$\frac{1}{2.89}$	$\frac{1}{11.47}$
	400	C_W	5.00	3.87	15.45	$\frac{1}{3.35}$	$\frac{1}{9.81}$
15 cm	400	B_W	2.72	2.72	0	$\frac{1}{1.41}$	$\frac{1}{4.86}$
	400	C_W	2.12	2.12	0	$\frac{1}{2.29}$	$\frac{1}{5.80}$
	400	D_W	1.84	1.84	0	$\frac{1}{2.98}$	$\frac{1}{7.04}$

The computed drift current in the case of r. p. m. 400 of blower is very large. In Table—7 L means the wave length corresponding to $(\overline{f}_{zero\ up\text{-}cross})$. $H^{1/3}/L$ is something similar to the representative wave steepness, and it is very large in the case of depth 15cm (r. p. m. 400 of blower). In this case the breaking of wave crest is visually observed. In the case of water depth 3cm the breaking of waves is not observed, and wave crests are covered by capillary waves. The similar treatment shows that waves used experimentally in Paper (I)

have $H^{1/3}/L = \frac{1}{11.69} \sim \frac{1}{13.83}$ (waves generated by r. p. m. 300 of blower) and $\frac{1}{9.92} \sim \frac{1}{11.95}$ (waves generated by r. p. m. 400 of blower) at calm condition, and these waves did not break.

We have shown the general properties of air flows and wind waves in the present experiment. The more detailed consideration in the course of directional spectrum is not used in this paper, and in the next paragraph we modify the measured frequency spectrum to the spectrum in still water by making use of the same method.

§ 3. Properties of frequency spectra at the case of water depth 3 cm

The measurement of frequency spectra in this paper depends upon the method of heterodyne detection of analogue type as shown by T. Hamada (1963).

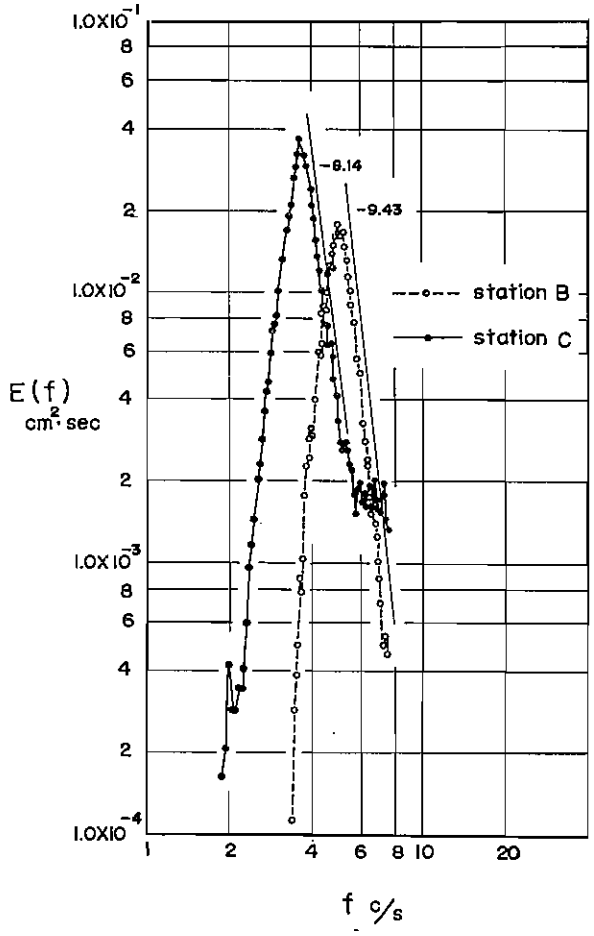

Fig—1 Spectrum intensity at B and C
(r. p. m. 200 of blower, water depth 3 cm)

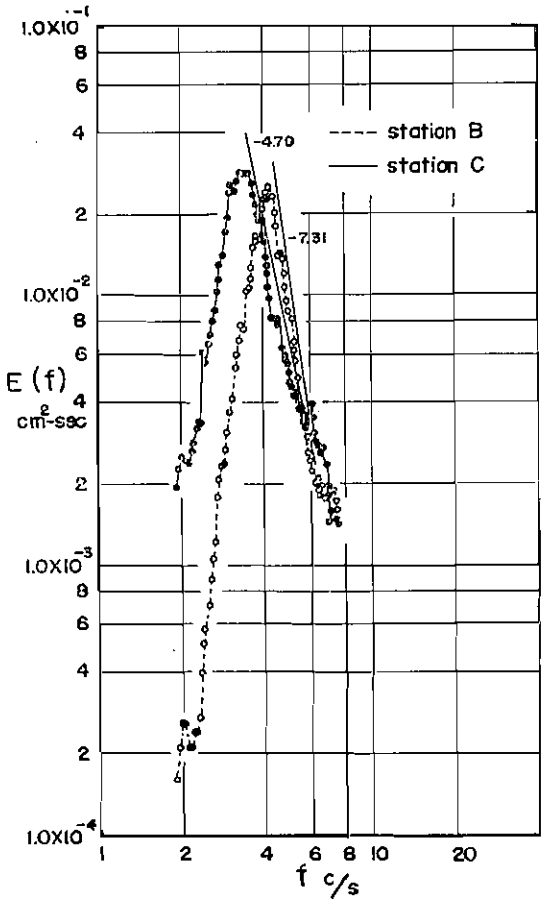

Fig—2 Spectrum intensity at B and C
(r. p. m. 300 of blower, water depth 3 cm)

Duration time of each measurement, x^2 —freedom of each spectrum, and the method of averaging these spectra at each cross sections are all same as in Paper (I). Spectra obtained in this way in the case of water depth of 3cm are shown in Fig—1, —2 and —3. Each figure corresponds to r. p. m. 200, r. p. m. 300 and r. p. m. 400 of air blower respectively. As spectra at station Bw and also at station Cw are recorded in the same figure, the tendency of development of the spectrum intensity of wind waves caused by the fetch length between station Bw and station Cw is clearly recognized.

The property of development of the spectrum intensity at the low frequency part is very similar in these figures, but the change of the spectrum intensity at the high frequency part reveals the explicitly different tendency in each figure. In Fig—1 $n = 8 \sim 9.5$ at the expression $E(f) \sim f^{-n}$ of the high frequency part is consistent, and, inspite of the tendency of rapid development of the low

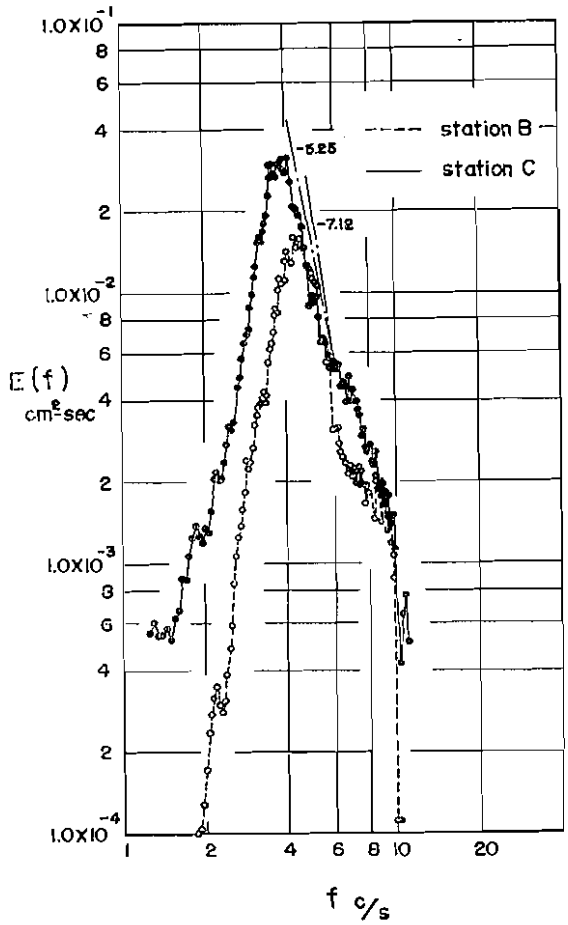

Fig—3 Spectrum intensity at B and C
(r.p.m. 400 of blower, water depth 3 cm)

frequency part, the acute attenuation is observed at the high frequency part. In Fig —2 n=5~7.5 at $E(f)\sim f^{-n}$ is noticed. The tendency of attenuation at the high frequency part of the spectrum is same as in Fig—1, but it is not so strong. In Fig—3 n is 5~7 at $E(f)\sim f^{-n}$, and the attenuation at the high frequency part is almost disappeared. By this way the tendency is shown that the intensity of the high frequency part of the wave profile spectrum of wind waves reveals a peculiar behavior of attenuation in a certain relation with the value of n at the expression $E(f)\sim f^{-n}$ and this supports author's point of view expressed in Paper (I).

In the case of the depth of water 3cm, the influence of the drift current induced by wind upon the properties of the spectrum cannot be neglected. So the above-mentioned version should be re-examined using the frequency f_0 in still water. We simply use the relation (4), assuming U_U as 3 cm/sec, 6 cm/sec and 16 cm/sec corresponding to r. p. m. 200, r. p. m. 300, and r. p. m. 400 of air blower

respectively. In this case,

$$\overline{\eta^2} = \int_0^\infty E(f)\, df = \int_0^\infty E(f) \frac{df}{df_0} df_0 \qquad (5)$$

The analytical determination of $\frac{df}{df_0}$ is not easy in the consideration of the effect of surface tension and of the condition of finite depth of water to bottom, and we adopted the method of numerical computation.

$E(f_0)$ related f_0 is shown in Fig—4. The behavior of the high frequency part of the spectrum related to the value of n in this case is not different from that in Fig—1, —2 and —3.

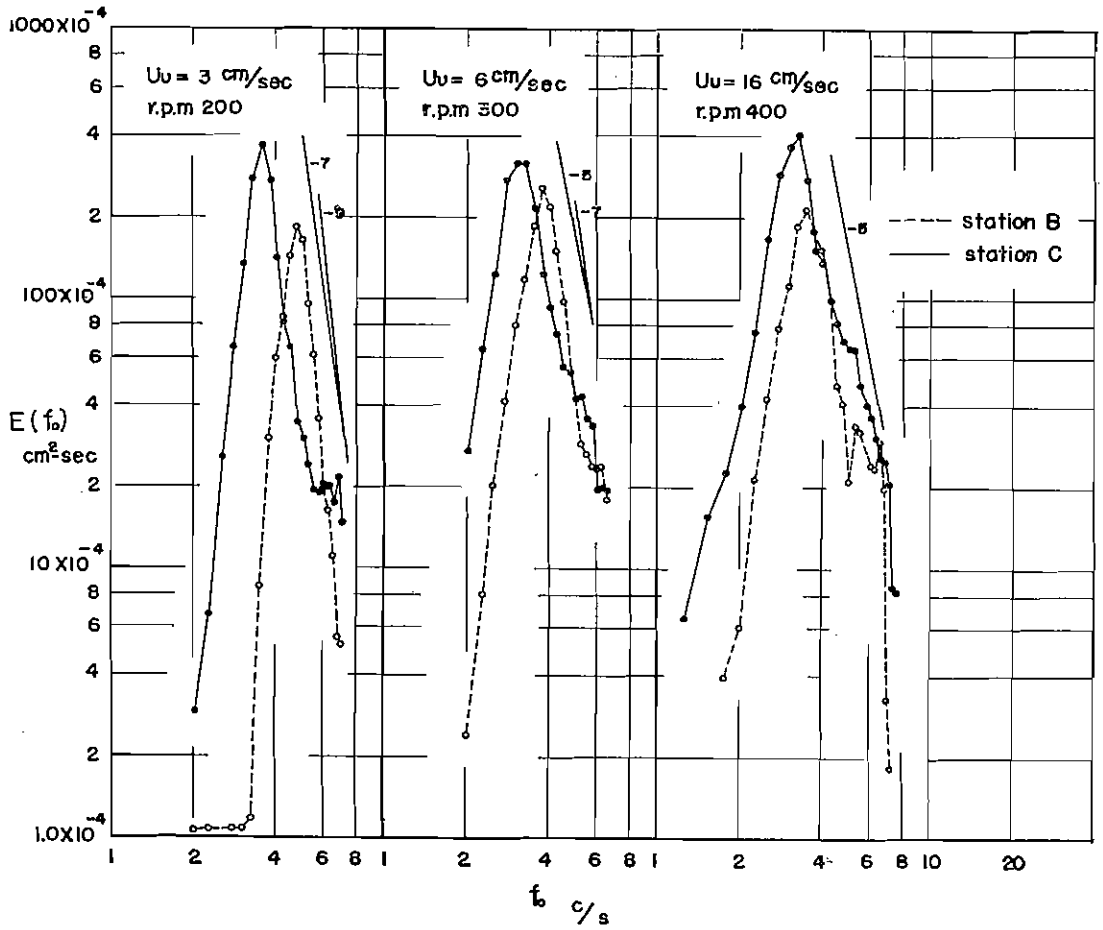

Fig—4 Spectrum intensity at *B* and *C* using the modified frequency in still water (water depth 3 cm)

§ 4, A property of the attenuation coefficient of high frequency part of the spectrum

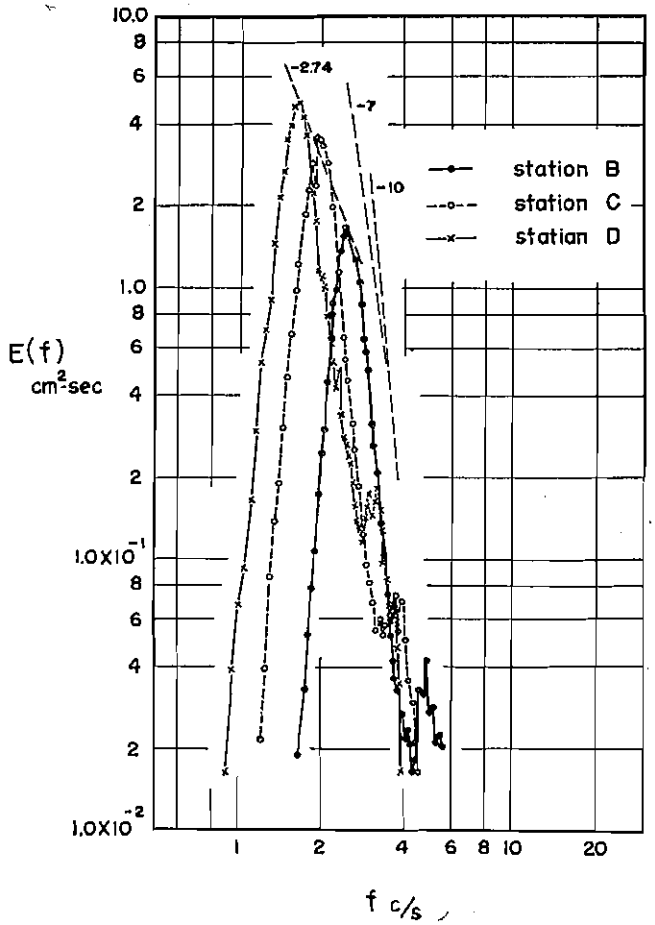

Fig—5 Spectrum intensity at B, C and D
(r. p. m. 400 of blower, water depth 15 cm)

The frequency spectra of wind waves under direct wind action are obtained in a case of depth of water 15 cm at r. p. m. 400 of blower, and are shown in Fig—5. They are obtained at stations Bw, Cw and Dw. The distances between Bw and Cw and between Cw and Dw are 900 cm equally.

In Fig—5 n is $7.7 \sim 10$ at the expression $E(f) \sim f^{-n}$ of the high frequency part, and the same tendency of rapid attenuation as those in Fig—1 is clear. On the other hand Fig—4 and —5 of Paper (I) indicate the tendency of attenuation of the high frequency part in the spectra of wind-generated waves which progress in a calm air condition without surface breaking. The depth of water to bottom is also 15 cm in that case.

As the values of n in Fig— 5 of this paper and in Fig— 4 and — 5 of Paper (I) are very similar, we may examine the tendency of attenuation at the high frequency part using these two data. The following coefficient is used. Its application is limited to the high frequency part which attenuates with the progress of waves.

$$\frac{E(f)_{(1)}-E(f)_{(2)}}{E(f)_{(2)}\,x} \qquad (6)$$

Here x means the distance of two stations for measurement, and E (f) at $x=o$ is designated to $E\ (f)_{(0)}$. $E\ (f)_{(1)}$ is the actually attenuated spectrum at $x=x$, and $E\ (f)_{(2)}$ is the assumed spectrum attenuated by molecular viscosity only. The effect of angular spreading is neglected. Accordingly,

$$\left.\begin{aligned} E(f)_{(1)} &= E(f)_{(0)}\ e^{-\alpha_1(\nu)x-\alpha_2 x} \\ E(f)_{(2)} &= E(f)_{(0)}\ e^{-\alpha_1(\nu)\,x} \end{aligned}\right\} \qquad (7)$$

$$\frac{E(f)_{(1)}-E(f)_{(2)}}{E\ (f)_{(2)}\ x}=\frac{e-\alpha_2 x-1}{x}\fallingdotseq-\alpha_2 \qquad (8)$$

Therefore the coefficient (6) is the attenuation coefficient in the relation with the travelling distance of wave energy in the case when the attenuation given by viscosity is eliminated. $E(f)_{(0)}$ and $E(f)_{(1)}$ are measured directly in experiment. $E(f)_{(2)}$ can be computed from $E(f)_{(0)}$ by the relations (31) and (32) of Paper (I). The coefficient (6) obtained by this way is recorded in Fig— 6 . To see the general tendency of this coefficient, the frequency of the spectrum peak in each case is also recorded in the same figure.

According to this figure,

(i) The maximum of the absolute value of the attenuation coefficient (6) has similar values in both cases of direct wind effect and of no wind effect. The value is $7\times10^{-4}\sim10\times10^{-4}$ in cm^{-1}.

(ii) The form of distribution of coefficient (6) is also similar in both cases. In the case when the wind blows directly on water surface in the present experiment, we can see visually the existence of surface breaking and the appearance of well developed capillary waves. On the contrary, when the wave is preserved at a calm condition in experiment of Paper (I), we see only the weak capillary wave on wave surface. Stillmore wind may be somewhat effective to develop the wave components even in the high frequency part of the spectrum. The conditions are so different in both cases. Nevertheless we obtained the above-mentioned result.

Although the present experiment is a limited example at a model waterway, it may be probable that the most important factor which controlls the attenuation

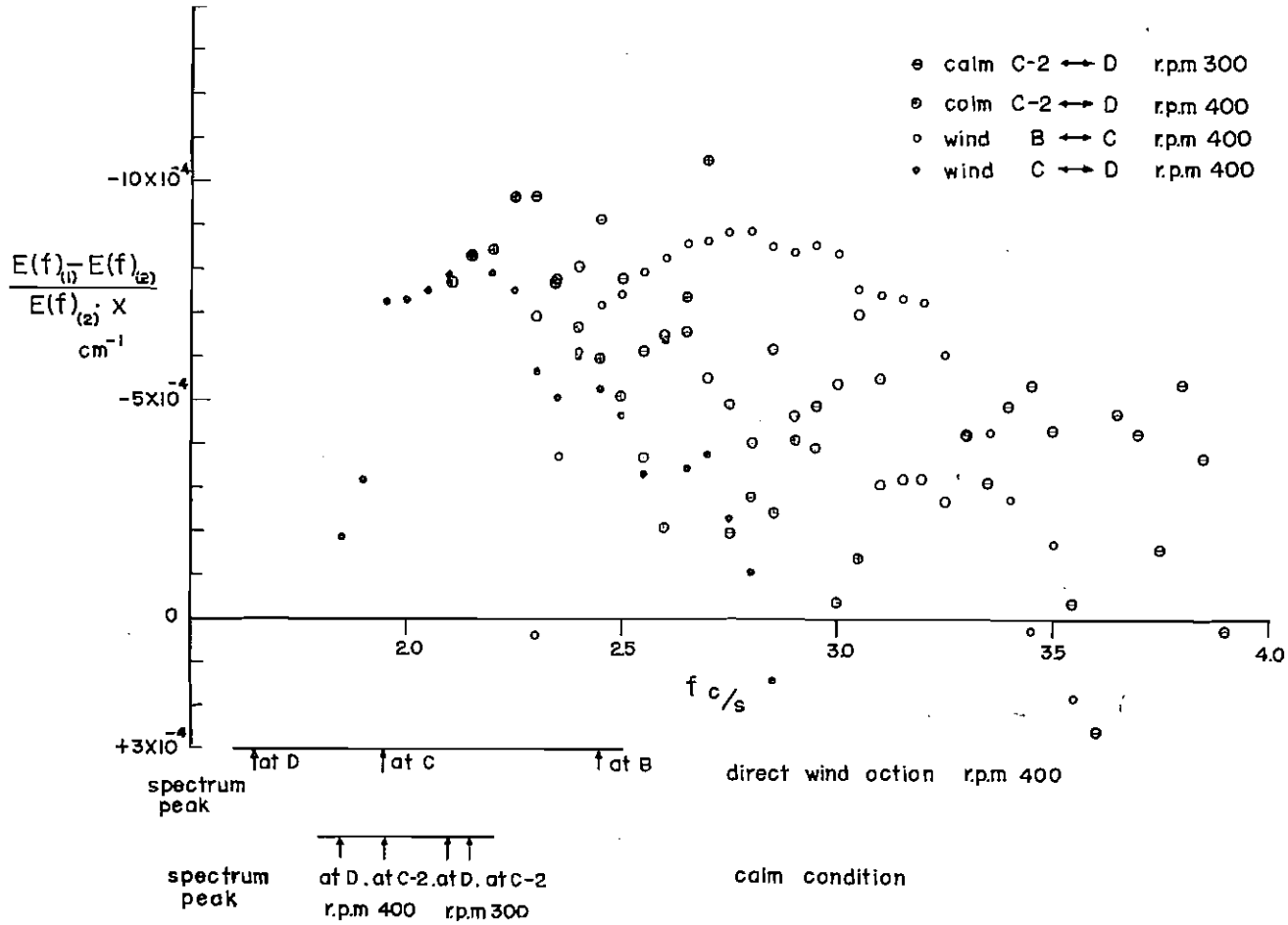

Fig—6 Distribution of attenuation coefficient $\frac{E(f)_{(1)}-E(f)_{(2)}}{E(f)_{(2)}\cdot x}$

of the intensity of high frequency part of the frequency spectrum of wind waves and of wind-generated waves is the value of n at the expression of $E(f) \sim f^{-n}$. Of course this is related with the case of deep water or approximately deep water, and $n \geqq 5$ is consistent.

The author is grateful to Mr. H. Kato who made a measurement of air flow, and also to members of our laboratory for their helps in experiment and in numerical computations.

Additional note: In this experiment we could not find the spectrum which has n clearly smaller than 5 at the high frequency part. It is doubtful that we may find the case of $n < 5$ in deep water or in approximately deep water with no undesirable regulation.

References

Hamada, T. 1963 An experimental study of development of wind waves. Report No. 2, Port and Harbour Research Institute, Japan.

Hamada, T. 1964 On the f^{-5} law of wind-generated waves. Report No. 6, Port and Harbour Research Institute, Japan.

(Received by the Institute, June 18, '66.)